TecnoLógicas

Geospatial Multi-Criteria Assessment of Soil Organic Matter Loss Vulnerability in a Tropical Watershed

Evaluación geoespacial multicriterio de la vulnerabilidad a la pérdida de materia orgánica del suelo en una cuenca hidrográfica tropical

Clever G. Becerra-Romero[1]; Andrés F. Echeverri-Sánchez[2];
Jhony A. Benavides-Bolaños[2]; María del M. Carreño-Sánchez[3]

[1]Corporación Autónoma Regional del Valle del Cauca, Cali – Colombia
[2]Escuela EIDENAR, Universidad del Valle, Cali – Colombia
[3]Universidad Federal de Viçosa, Viçosa – Brasil

Correspondence: clever-gustavo.becerra@cvc.gov.co

Received: 15 November 2025 **Accepted:** 22 September 2026 **Available:** 28 September 2026

How to cite / Cómo citar

C. G. Becerra-Romero, A. F. Echeverri-Sánchez, J. A. Benavides-Bolaños and M. del M. Carreño-Sánchez, "Geospatial Multi-Criteria Assessment of Soil Organic Matter Loss Vulnerability in a Tropical Watershed" *TecnoLógicas*, vol. 29, no. 67, e3762, 2026.
https://doi.org/10.22430/22565337.3762

CC BY NC SA

Abstract

Soil organic matter (SOM) supports fertility, aggregation, water retention, and carbon storage. Therefore, mapping its vulnerability is crucial in tropical watersheds under intensive agriculture. In Colombia, few spatially explicit and operational frameworks integrate intrinsic soil properties and climatic-topographic factors into a single expert-weighted index. This study aimed to operationalize and apply a multi-criteria index based on Geographic Information System (GIS) and Analytic Hierarchy Process (AHP): the Soil Organic Matter Loss Vulnerability Index (SOM-LVI) to assess spatial vulnerability to SOM loss in the Tuluá and La Paila river watersheds, Valle del Cauca, Colombia. The methodology employed consisted of integrating six parameters weighted through AHP: clay content, slope, Holdridge life zones, temperature, precipitation, and soil pH, using 1:25000 cartography and raster layers of climate and relief. SOM-LVI values ranged from 0.19 to 0.79 across 135426 ha. The results showed that the High (49.6%) and Moderate (41.0%) vulnerability classes jointly represented 90.6% of the study area, while low vulnerability covered 9.4%. Spatially, hotspots were concentrated in middle and lower sectors on dissected reliefs, whereas forested headwaters showed lower vulnerability. High vulnerability predominated within Alfisols and Mollisols, whereas Andisols, Inceptisols, and Histosols were predominantly classified as Moderate or Low. Finally, it is concluded that the SOM-LVI provides a replicable methodology for prioritizing management practices that protect SOM where vulnerability is greatest, although its application depends on available cartography, expert weights, and the underlying climatic and topographic variables.

Keywords

Geographic information systems, holdridge life zones, soil organic matter, soil properties, tropical watershed.

Resumen

La materia orgánica del suelo (MOS) sustenta la fertilidad, agregación, retención de agua y almacenamiento de carbono. Por lo tanto, mapear su vulnerabilidad resulta crucial en cuencas tropicales bajo agricultura intensiva. En Colombia existen pocos marcos espaciales explícitos y operativos que integren propiedades intrínsecas del suelo y factores climáticos-topográficos en un único índice ponderado por expertos. Esta investigación tuvo como objetivo operacionalizar y aplicar un índice multicriterio basado en sistemas de información geográfica y el Proceso de Análisis Jerárquico (PAJ): el Índice de Vulnerabilidad a la Pérdida de Materia Orgánica del Suelo (IVP-MOS) para evaluar la vulnerabilidad espacial a la pérdida de MOS en las cuencas hidrográficas de los ríos Tuluá y La Paila, Valle del Cauca, Colombia. La metodología empleada consistió en integrar seis parámetros ponderados mediante PAJ: contenido de arcilla, pendiente, zonas de vida de Holdridge, temperatura, precipitación y pH del suelo, utilizando cartografía 1:25000 y capas ráster de clima y relieve. Los valores del IVP-MOS oscilaron entre 0.19 y 0.79 en 135426 ha. Los resultados obtenidos mostraron que las clases de vulnerabilidad alta (49.6 %) y moderada (41.0 %) representaron el 90.6 % del área, mientras que la vulnerabilidad baja cubrió el 9.4 %. Espacialmente, los puntos críticos se concentraron en sectores medios e inferiores sobre relieves disectados, mientras que las cabeceras boscosas presentaron menor vulnerabilidad. La vulnerabilidad alta predominó dentro de los Alfisoles y Molisoles, mientras que los Andisoles, Inceptisoles e Histosoles presentaron principalmente vulnerabilidad moderada o baja. Finalmente, se concluye que el IVP-MOS proporciona una metodología replicable para priorizar prácticas de manejo que protejan la MOS donde la vulnerabilidad es máxima, aunque su aplicación depende de la cartografía disponible, los pesos expertos y las variables climáticas y topográficas subyacentes.

Palabras clave

Sistemas de información geográfica, zonas de vida de holdridge, materia orgánica del suelo, propiedades del suelo, cuenca hidrográfica tropical.

1. INTRODUCTION

Soil organic matter (SOM) is a foundational regulator of soil functioning in agricultural landscapes, governing aggregate formation and stability, pore connectivity, water- and nutrient-holding capacity, and the energy base for microbial networks that drive biogeochemical cycling. SOM serves as a critical determinant of soil fertility, structural stability, water retention capacity, and climate-relevant carbon storage, underpinning multiple essential pedological processes through mechanisms that include the provision of substrate for microbial metabolism, chelation and buffering of soil cations, regulation of nutrient cycling and availability [1], [2], [3]. The carbon contained within SOM pools exists in multiple forms—from labile, readily decomposable fractions that fuel immediate microbial processes, to recalcitrant, stable fractions that persist in soils for centuries—reflecting a continuum of chemical complexity and biological accessibility [4], [5], [6]. At the mechanistic level, SOM interacts with the mineral matrix through organo-mineral complexes, wherein dissolved organic matter adsorbs onto clay surfaces, iron and aluminum oxide coatings, and other reactive mineral phases, effectively sequestering carbon from decomposer communities and increasing its residence time in soil [7], [8], [9], [10]. Across scales, mechanisms that protect organic carbon within organo-mineral associations and aggregates determine the residence time of SOM, thereby mediating both agronomic performance and climate-relevant carbon stocks [11]. In fine-textured soils, clay-mediated sorption and microaggregate occlusion physically shield organic substrates from enzymatic attack; in coarser textures, limited surface reactivity and aeration accelerate turnover [11]. Because these controls co-vary with terrain, climate, and management, the spatial distribution of SOM and its vulnerability to loss cannot be inferred from single indicators alone.

The loss of SOM in working lands is a pervasive outcome of land conversion, disturbance, and management intensification, with consequences for yield stability, input efficiency, and off-site impacts such as erosion and water-quality impairment. SOM decline has been documented as one of the most widespread and consequential forms of soil degradation across diverse agroecosystems [12], [13], [14], [15]. In tropical valleys such as those in Valle del Cauca, Colombia, SOM degradation is particularly acute: high mean annual temperatures (15–24 °C), coupled with favorable soil moisture regimes and intensive agricultural management practices, create conditions that accelerate organic matter mineralization through enhanced microbial respiration

and reduced carbon sequestration [16]. Even within established production regions, recent work in this inter-Andean agricultural watershed demonstrates that soil organic carbon varies systematically with soil order, texture, slope, and microclimate—underscoring how pedo-climatic context structures vulnerability patterns at management scales [16]. The economic consequences of SOM loss are substantial and multifaceted: a reduction of 1% in soil organic carbon can result in crop productivity declines of 5–15%, depending on crop type and climate conditions, while simultaneously requiring increases in synthetic fertilization costs of 50–200 USD ha^{-1} annually to maintain yields [17]. Beyond immediate productivity impacts, SOM loss reduces soil structural stability, increases erodibility, diminishes water retention capacity, suppresses biological diversity, and reduces the carbon sequestration potential of soils—thereby compromising multiple ecosystem services simultaneously [18].

Geographic Information Systems (GIS) coupled with multi-criteria decision analysis (MCDA) frameworks, particularly the Analytic Hierarchy Process (AHP), offer a transparent means to integrate intrinsic soil properties and extrinsic drivers into spatial indices that support targeting and policy [19], [20]. The MCDA methodology operates by identifying and weighting multiple biophysical, climatic, and topographic parameters that collectively determine soil susceptibility to specific degradation processes, then integrating these parameters through simple additive weighting (SAW) or other aggregation functions to produce spatially continuous vulnerability surfaces [21], [22], [23]. When employed for parameter weighting, AHP provides a transparent, reproducible mechanism for translating expert knowledge and scientific literature into quantitative weights that reflect the relative importance of each parameter in driving vulnerability [24]. In GIS-MCDA applications, criterion harmonization occurs through common-scale normalization, enabling reproducible overlay analysis and interpretable thresholds [25], [26]. However, despite the demonstrated utility of such frameworks in mapping physical soil degradation processes, the application of spatially explicit MCDA-GIS approaches to assess SOM loss vulnerability remains underdeveloped in tropical Latin American contexts. Existing GIS-MCDA applications for soil degradation, erosion, land suitability, and environmental vulnerability provide useful methodological precedents; however, few operational indices explicitly integrate soil, terrain, and climatic controls to prioritize vulnerability to SOM loss in tropical agricultural watersheds.

This study aimed to operationalize and apply a GIS- and AHP-based multi-criteria index—the Soil Organic Matter Loss Vulnerability Index (SOM-LVI)—to assess spatial vulnerability to SOM loss in the Tuluá and La Paila river watersheds, Valle del Cauca, Colombia. The index integrates six AHP-weighted edaphic, topographic, and climatic parameters—clay content, terrain slope, Holdridge life zones, mean annual temperature, mean annual precipitation, and soil pH—through GIS-based simple additive weighting across 135426 ha. The resulting vulnerability surface was analyzed by soil taxonomic order and agrological class to identify priority soil–landscape combinations for SOM conservation. We hypothesized that higher vulnerability would occur in warmer mid- and lower-watershed sectors where moderate clay contents, near-neutral pH, and undulating-to-steep terrain coincide, whereas cooler headwater areas dominated by soils with greater organic matter protection would show lower vulnerability. We also expected Moderate and High vulnerability to overlap substantially with agrological classes of high productive importance, revealing areas where SOM conservation is particularly relevant for agricultural planning.

2. METHODOLOGY

We employed a spatially explicit vulnerability workflow that fuses MCDA, AHP, and GIS. This integration enables consistent weighting, normalization, and aggregation of qualitative and quantitative indicators across space, supporting comparable, map-ready outputs. Comparable hybrids of MCDA–AHP–GIS have been successfully deployed in a wide range of environmental applications [20], [27], [28], [29].

2.1 Study area

The study area is located in the Department of Valle del Cauca, southwestern Colombia, and spans several municipalities. The largest jurisdictions are Guadalajara de Buga (40971.16 ha), Tuluá (37533.31 ha), and Bugalagrande (16730.45 ha), followed by Sevilla (15221.91 ha), Zarzal (11990.67 ha), San Pedro (6902.88 ha), and El Cerrito (6141.09 ha). By contrast, Bolívar, Ginebra, and Riofrío include smaller fractions (<1 ha). Hydrologically, the area comprises the Tuluá watershed (91577.70 ha) and the La Paila–Sevilla (31278.26 ha), La Paila–Zarzal (11990.67 ha), and La Paila–Bugalagrande (674.09 ha) watersheds (Figure 1).

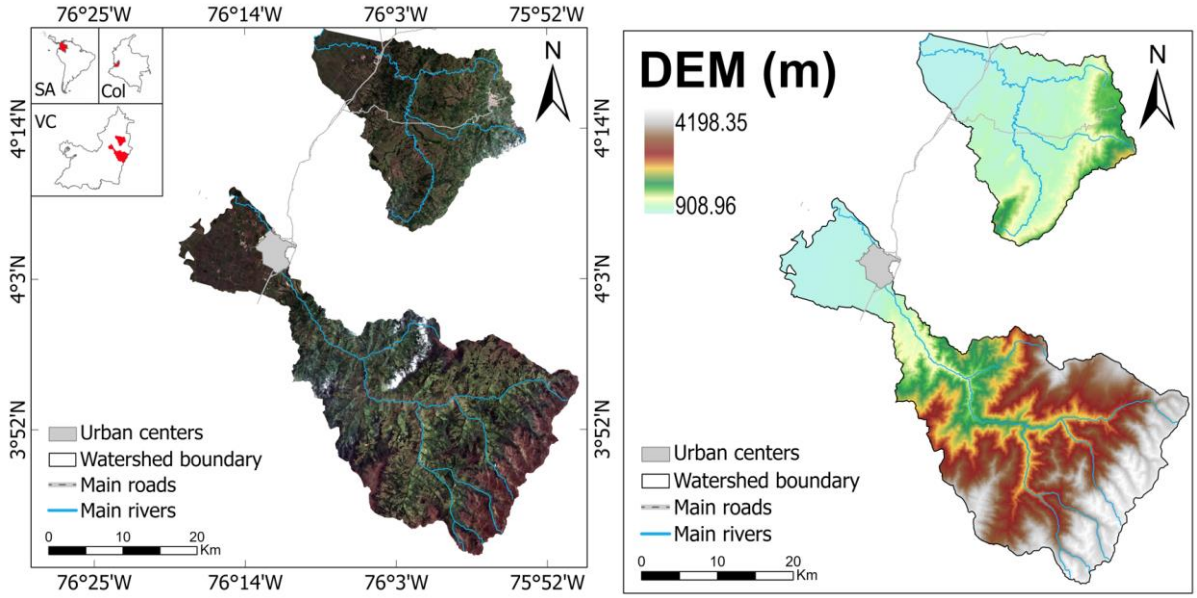


Figure 1. Study area. Left: true color composite; right: Digital elevation model (DEM); (SA: South America, Col: Colombia, VC: Valle del Cauca). Source: own elaboration.

Across the prioritized watersheds, annual rainfall spans roughly 881–2210 mm, with most of the area concentrated between 1200 mm and 1600 mm; this hydroclimatic setting reflects the inter-Andean gradient typical of the region. Mean temperatures exceed 15 °C approximately over two-thirds of the landscape, with smaller montane tracts in the 10–15 °C and 5–10 °C bands. Valle del Cauca's semidetailed soil survey (1:25000) indicates a landscape composed of Alfisols, Andisols, Entisols, Histosols, Inceptisols, Mollisols, and Vertisols—Andisols concentrated at higher, cooler elevations; Mollisols and Alfisols prevailing in intensively farmed low- to mid-elevation terrain; Inceptisols and Entisols occupying transitional geomorphic positions; Histosols occurring locally in poorly drained settings; and Vertisols associated with shrink–swell parent materials [30].

2.2 Parameters definition and weighting

Drawing on a focused literature review, local data and the outcomes of an expert workshop with representatives from CIAT, CVC, Cenicaña, Universidad del Valle, Universidad de Caldas and Universidad Nacional de Colombia, we identified six vulnerability parameters available for the Valle del Cauca: clay content, slope, Holdridge life zones, mean annual temperature, mean annual precipitation, and soil pH (Table 1). Selection prioritized variables supported by the 1:25000 soil survey [30] and freely available local geodatasets via the GeoCVC-Advanced visor portal to ensure territorial validity and data availability.

Table 1. Description of vulnerability parameters (Clay: clay content; SL: slope; HLZ: Holdridge life zones; T: temperature; PR: precipitation; pH: soil pH). Source: own elaboration.

Parameter	Description	Format
Clay	Clay reflects a soil's mineral surface area and reactivity, which governs mineral-associated organic matter (MAOM) formation and the physical inaccessibility of C to microbes; higher reactive clay generally increases SOC protection and residence time. Because small shifts in clay (and associated surface area) can markedly change MAOM saturation deficits and SOC persistence, this parameter carries the highest weight [31], [32], [33].	Vector
SL	Slope captures the propensity for runoff, detachment, and downslope redistribution of the SOC-rich surface horizon; steeper terrain accelerates lateral C export and shortens SOC residence time. Given its direct control on physical loss pathways, slope justifies a high weight comparable to other primary drivers [34], [35], [36].	Raster
HLZ	Holdridge life zones integrate biotemperature and precipitation, serving as a bioclimatic proxy for primary productivity (C inputs) and for climatic controls on SOC stabilization potential; zones with warmer, drier regimes tend to support lower SOC persistence than cooler, wetter ones. This integrative climatic context merits a substantial weight to modulate edaphic and topographic effects [37], [38].	Vector
T	Temperature regulates microbial activity and decomposition rates; warming consistently reduces SOC stocks, especially in surface/mineral-associated pools. Its effect is strong but interacts with moisture and mineral protection, so we assign an intermediate weight [39], [40].	Raster
PR	Precipitation influences soil moisture, plant productivity (C inputs), leaching, aggregate dynamics, and erosive transport; higher or more intense rainfall can alter aggregation and SOC retention, while broad MAP gradients co-vary with SOC at regional scales. Because part of moisture/topographic effects is captured elsewhere, precipitation receives an intermediate weight [41], [42].	Raster
pH	Soil pH modulates microbial communities and exoenzyme function and thus mineralization efficiency; near-neutral pH generally favors faster SOM turnover relative to acidic extremes. As a biochemical regulator secondary to the dominant physical/climatic drivers, pH is assigned to lower weight [43], [44].	Vector

2.3 Parameters categorization

Each parameter was discretized into ordered vulnerability classes using parameter-specific thresholds derived from literature, expert elicitation, and the empirical distribution of the data. This harmonized scale enables direct cross-parameter comparability and a consistent, reproducible assessment within the SOM-LVI. Normalized values are summarized in Table 2.

2.4 GIS analysis

Vector soil information (clay, pH, and life zones) was dissolved and rasterized; climatic surfaces were prepared and, where required, interpolated by ordinary kriging; slope was derived from the Digital Elevation Model (DEM); and all rasters were normalized and aligned using Mask/Snap Raster prior to index calculation. All resulting rasters were harmonized to a spatial resolution of 100 m. Parameters were combined in the SOM-LVI as a weighted linear sum, with weights established and applied uniformly across the study area. The resulting vulnerability surface was then intersected with agrological classes and soil taxonomic orders to aid interpretation and assess consistency with land capability patterns in the Tuluá–La Paila watershed systems. All spatial processing was conducted in ArcGIS Pro version 3.4.1 using the EPSG: 3115 coordinate reference system. The final raster stack was harmonized to a 100 m cell size using a common mask, extent, snap raster, and cell alignment before map algebra. Continuous layers were resampled using bilinear interpolation, whereas categorical or reclassified layers were resampled using nearest neighbor. Temperature and precipitation

were interpolated using ordinary kriging; however, nugget, sill, and range values are not reported because no formal variogram report was retained. Parameter weights were derived from expert elicitation using an AHP-based prioritization logic, but no pairwise comparison matrix or consistency ratio was retained; therefore, the index is interpreted as an expert-weighted MCDA prioritization tool.

Table 2. Normalized values by parameter and category (Clay: clay content; SL: slope; HLZ: Holdridge life zone; T: temperature; PR: precipitation; pH: soil pH; NV: normalized value). Source: own elaboration.

Parameter	Vulnerability	Categories	NV
Clay	Very high	< 10	1.0
	High	10–20	0.8
	Moderate	20–35	0.6
	Low	35–60	0.4
	Very low	> 60	0.2
SL	Very high	> 100	1.0
	High	50–100	0.8
	Moderate	12–50	0.6
	Low	3–12	0.4
	Very low	< 3	0.2
HLZ	Very high	Tropical Desert; Subtropical Desert	1.0
	High	Tropical dry forest, Premontane dry forest, Lower montane dry forest	0.8
	Moderate	Premontane moist forest, Montane moist forest, Lower montane moist forest	0.6
	Low	Premontane wet forest, Montane wet forest, Lower montane wet forest	0.4
	Very low	Subalpine rain páramo	0.2
T	Very high	> 20	1.0
	High	15–20	0.8
	Moderate	10–15	0.6
	Low	5–10	0.4
	Very low	< 5	0.2
PR	Very high	< 400	1.0
	High	400–800	0.8
	Moderate	800–1200	0.6
	Low	1200–1600	0.4
	Very low	> 1600	0.2
pH	Very high	6.0–7.5	1.0
	High	7.5–8.5	0.8
	Moderate	5.0–6.0	0.6
	Low	> 8.5	0.4
	Very low	< 5.0	0.2

2.5 SOM-LVI integration

The SOM-LVI was computed using SAW within a MCDA framework, where each parameter was normalized to [0, 1] and combined as a weighted linear sum with weights summing to 1, as described in previous work [45], [46], [47]. Urbanized, sealed surfaces were masked out prior to calculation. The SAW procedure was implemented on a set of normalized raster layers to generate spatially explicit vulnerability scores, which were subsequently mapped to depict gradients in vulnerability to SOM loss across the study area. The general model form is shown in (1).

$$\mathrm{SOM-LVI} = \sum_{i=1}^{n} (w_i \times \mathrm{VN}_i) \tag{1}$$

In (1), w_i denotes the weight assigned to each vulnerability parameter i, and VN_i corresponds to the normalized value of that parameter. The formulation of the index is shown in (2):

$$\mathrm{SOM-LVI} = [(0.25 \times \mathrm{Clay}) + (0.19 \times \mathrm{SL}) + (0.19 \times \mathrm{HLZ}) + (0.14 \times \mathrm{T}) + (0.14 \times \mathrm{PR}) + (0.09 \times \mathrm{pH})] \tag{2}$$

The general workflow used in this research is described in Figure 2.

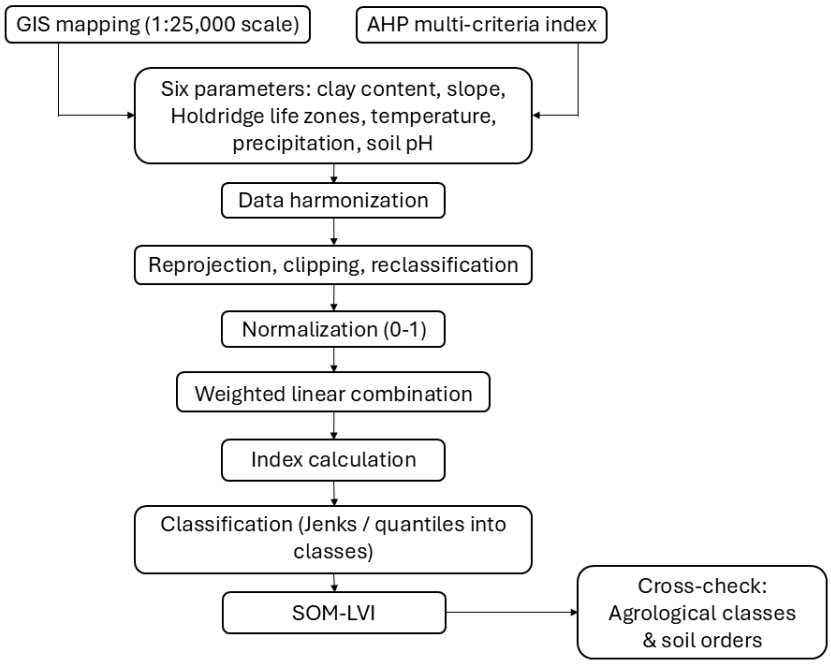


Figure 2. Workflow used to calculate the SOM-LVI. Source: own elaboration.

3. RESULTS AND DISCUSSION

3.1 Normalized parameter maps

The normalized vulnerability parameter maps are presented in Figure 3.

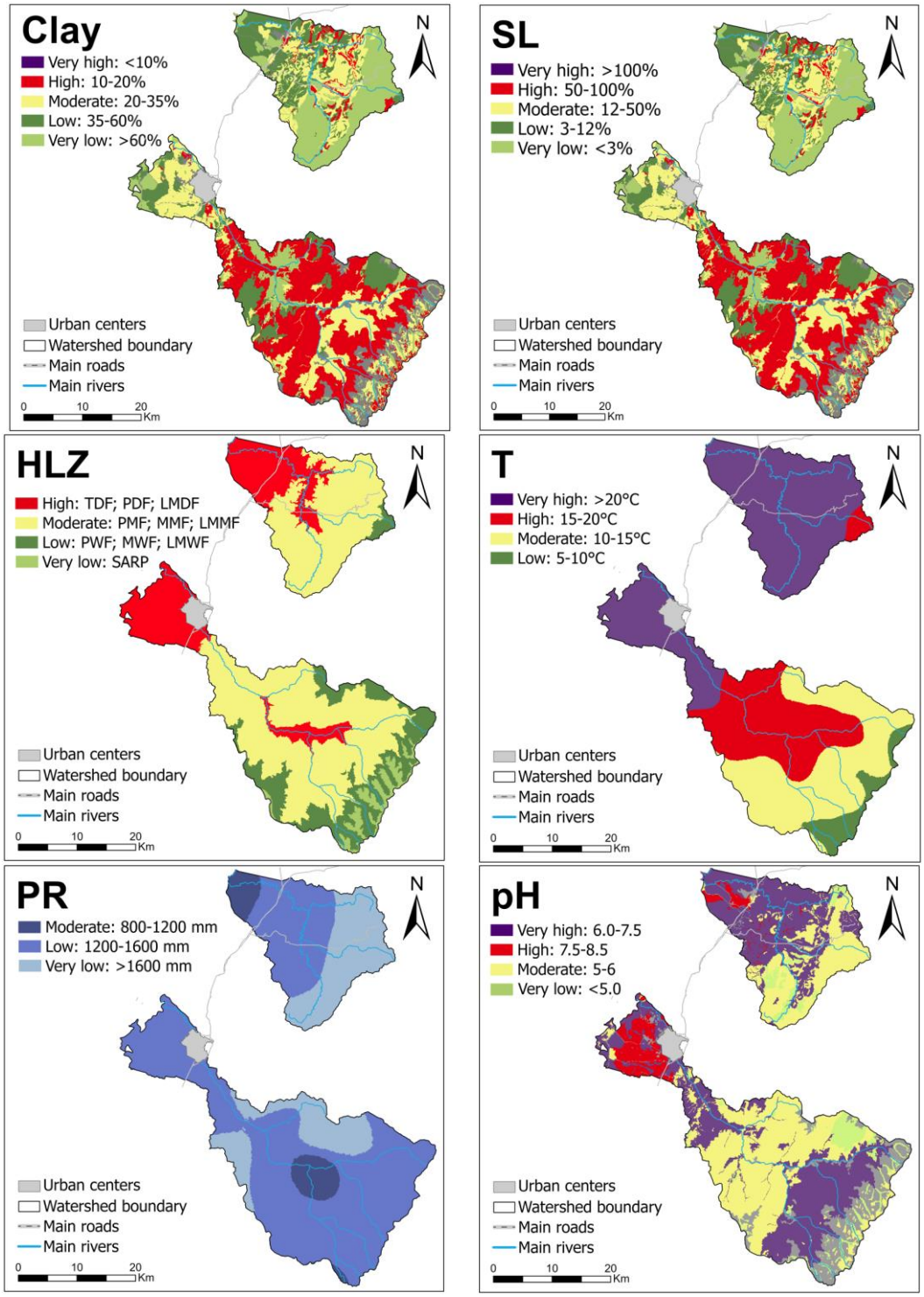


Figure 3. Normalized vulnerability parameter maps: a) Clay: clay content; b) SL: slope; c) HLZ: Holdridge life zones (TDF: Tropical dry forest; PDF: Premontane dry forest; LMDF: Lower montane dry forest; PMF: Premontane moist forest; MMF: Montane moist forest; LMMF: Lower montane moist forest; PWF: Premontane wet forest; MWF: Montane wet forest; LMWF: Lower montane wet forest; SARP: Subalpine rain páramo); d) T: temperature; e) PR: precipitation; f) pH: soil pH. Source: own elaboration.

3.2 Homogeneous vulnerability zones

The SOM-LVI classifies 135426 ha into four vulnerability classes. High vulnerability predominates, encompassing 67207 ha (49.6%), followed by Moderate with 55464 ha (41.0%); Low accounts for 12752 ha (9.4%), while Very High and Very Low are negligible (≈0%). Taken together, High and Moderate cover >90% of the study area, indicating widespread susceptibility to SOM loss. Spatially, the highest vulnerability clusters in the middle–lower portions of the Tuluá and La Paila watersheds—especially in Tuluá, San Pedro, and Buga—where undulating to steep relief, higher slopes, and fragmented agricultural cover coincide. Lower vulnerability is concentrated in upper, forested sectors (e.g., Sevilla and Ginebra), consistent with cooler temperatures and more continuous vegetation that favor SOM accumulation. The SOM-LVI ranges from 0.19 to 0.79 across the landscape, reflecting the low-to-high spectrum of susceptibility (Figure 4).

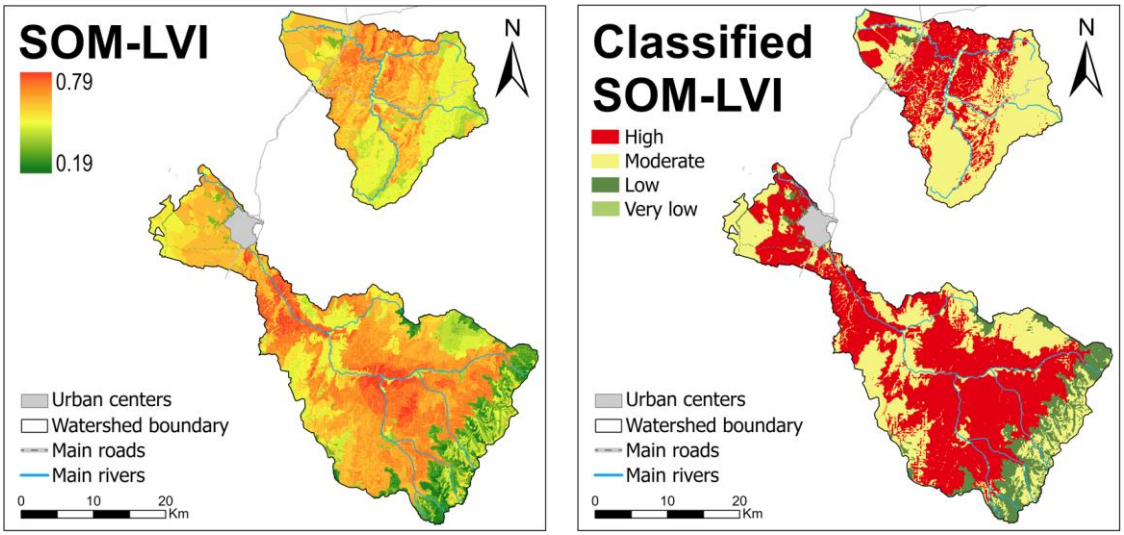


Figure 4. SOM-LVI integration; left: SOM-LVI; right: classified SOM-LVI. Source: own elaboration.

Across the 135426 ha study area, the SOM-LVI assigned 9.4% of the landscape to Low, 41.0% to Moderate, and 49.6% to High vulnerability. Very Low vulnerability accounted for only 3 ha and Very High vulnerability was not represented. The underlying parameters show contrasting area distributions, with temperature and pH dominated by Very High vulnerability, precipitation concentrated in Low vulnerability, and slope, Holdridge life zones, and clay mainly in Moderate to High categories (Table 3).

Table 3. Area distribution in ha by the SOM-LVI based on edaphic, topographic, and climatic parameters (V: vulnerability; SL: slope; HLZ: Holdridge life zone; T: temperature; pH: soil pH; PR: precipitation; Clay: clay content). Source: own elaboration.

V	SL	HLZ	T	pH	PR	Clay	SOM-LVI	SOM-LVI %
Very low	21681	4946	0.0	8342	34102	28042	3	0.0
Low	15268	19992	6577	0.0	92421	21622	12752	9.4
Moderate	67401	79755	36080	48727	8955	32185	55464	41.0
High	30717	30823	31619	7387	0.0	41841	67207	49.6
Very high	421	0.0	61202	55596	0.0	41	0.0	0.0

When disaggregated by agrological class, Moderate and High SOM-LVI categories dominate classes 3–7, where they jointly account for 97.63–100.00 % of the area, while class 8

shows a more even distribution among Low (31.20%), Moderate (31.31%), and High (37.48%) vulnerability. Very Low vulnerability is virtually absent across all agrological classes (Table 4).

Table 4. Percentage distribution of areas by the SOM-LVI, disaggregated by agrological classes (V: vulnerability). Source: own elaboration.

V	Agrological classes					
	Class 3	Class 4	Class 5	Class 6	Class 7	Class 8
Very low	0.00%	0.00%	0.00%	0.00%	0.00%	0.01%
Low	0.97%	0.49%	0.00%	0.42%	2.37%	31.20%
Moderate	49.61%	53.20%	22.63%	53.35%	31.59%	31.31%
High	49.42%	46.31%	77.37%	46.23%	66.04%	37.48%

By soil taxonomic order, High SOM-LVI vulnerability is predominant in Alfisols (75.15%), Mollisols (74.51%), and Vertisols (46.37%), whereas Andisols, Entisols, and Inceptisols present a larger share of Moderate vulnerability (36.54–65.55%). Low vulnerability is substantial only in Histosols (74.21%) and Andisols (21.31%), and Very Low classes are absent across all soil orders (Table 5).

Table 5. Percentage distribution of areas by the SOM-LVI, disaggregated by soil taxonomic order (V: vulnerability). Source: own elaboration.

V	Soil order						
	Alfisol	Andisol	Entisol	Histosol	Inceptisol	Mollisol	Vertisol
Very low	0.00%	0.00%	0.00%	0.00%	0.00%	0.00%	0.00%
Low	0.08%	21.31%	2.51%	74.21%	1.29%	0.15%	0.90%
Moderate	24.77%	36.54%	62.53%	25.49%	65.55%	25.33%	52.74%
High	75.15%	42.14%	34.96%	0.30%	33.15%	74.51%	46.37%

3.3 Contrast with empirical studies and dominant controls

The SOM-LVI classified 49.6% of the study area as High vulnerability and 41.0% as Moderate vulnerability, with the highest values concentrated in warmer middle and lower watershed sectors and lower values occurring mainly in cooler headwaters. This spatial contrast is directionally consistent with field evidence from another inter-Andean agricultural area in Valle del Cauca, where cold-climate Andisols under secondary vegetation had the highest measured SOC stock (174.83 t ha^{-1}), whereas warm-climate Mollisols under cultivated pasture had the lowest (20.42 t ha^{-1}) [16]. The soil-order distributions obtained here show a comparable direction: High vulnerability represented 75.15% of Alfisols and 74.51% of Mollisols, while Andisols contained a substantially larger Low-vulnerability fraction. However, the two studies represent different types of evidence: the previous study measured SOC stocks, whereas the SOM-LVI maps potential vulnerability. Therefore, this correspondence supports the regional plausibility of the mapped gradient but does not constitute independent validation of the index.

The lower vulnerability mapped in upper, more continuously vegetated sectors and the higher vulnerability associated with dissected terrain are also consistent with empirical observations from other agricultural watersheds. Ewunetu et al. [48] found higher SOM under natural forest (3.93%) than under cultivated land (3.00%) and higher SOM on lower slopes (3.55%) than on upper slopes (2.70%). Although that study was conducted under different soils and climatic conditions, the direction of its results supports the contrast identified here between protected headwater environments and agricultural or sloping sectors. Similar field evidence of rapid SOC decline following forest-to-maize conversion in a tropical watershed further indicates that reduced vegetation inputs and soil disturbance can reinforce the inherent climatic and topographic vulnerability represented by the SOM-LVI [6]. These comparisons do not imply that

current land use caused the mapped classes because management was not included as an explicit index parameter; rather, they show that the spatial pattern is compatible with measured responses reported in tropical agricultural landscapes.

The mapped High-vulnerability areas appear to represent two different but spatially connected pathways. In relatively flat or gently undulating valley sectors, vulnerability is associated mainly with warm temperatures, near-neutral pH, and intermediate mineral protection, conditions that can favor rapid organic matter turnover [39], [43], [49], [50], [51]. On dissected hillsides, vulnerability is more directly related to the removal and redistribution of SOC-rich surface soil through runoff and erosion [34], [52], [53]. Conversely, cooler temperatures and the strong stabilization capacity of short-range-order minerals help explain the larger Moderate- and Low-vulnerability fractions found in some Andisol areas [54], [55]. Distinguishing these pathways is important because similar SOM-LVI values may reflect different dominant processes and, consequently, require different conservation responses.

3.4 Indicator behavior, weights, and mechanistic interpretation

The weight structure (clay = 0.25; slope = 0.19; Holdridge life zone = 0.19; temperature = 0.14; precipitation = 0.14; pH = 0.09) reflects contemporary understanding of SOC persistence. Clay is a first-order control on MAOM and on physical inaccessibility of substrates to decomposers; small shifts in clay (and thus in reactive surface area) can markedly change MAOM saturation deficits and SOC residence time [31], [32], [33]. Empirically, soils > 30% clay can store 2–3 times more C than sandy soils [56], [57], whereas clay contents below ~15% sharply reduce stabilization capacity [58].

Slope warrants a high weight because it directly governs the propensity for detachment, transport, and downslope redistribution of fine, C-rich particles [34]-[36]. Moderate-to-steep gradients (> 12%) accelerate shear stress and flow velocities, with documented 40–60% topsoil SOC differences between upper and lower slope positions and large increases in export with each 5% gradient increment [48], [59].

Holdridge life zones integrate temperature, precipitation, and evapotranspiration, providing a bioclimatic scaffold for expected C inputs (primary productivity) and climatic constraints on stabilization [37], [38]. In tropical humid zones, rapid mineralization of particulate OM (1–3 yr residence times) is common, whereas cooler temperate/montane zones show slower turnover (5–15 yr) despite lower productivity [60], [61]. Assigning life zones, a substantial weight thus allows climate to modulate edaphic and topographic signals coherently.

Temperature and precipitation receive intermediate weights because their effects, though strong, are partially mediated by moisture dynamics, substrate quality, mineral protection, and topographic convergence [39], [40], [41], [42]. Mean annual temperature exerts a well-documented control on decomposition (typical Q10 ≈ 1.5–2.5; higher for more recalcitrant fractions), with ~10–15% losses per +1 °C in C-rich soils under favorable moisture [60], [62], [63]. Precipitation governs soil moisture, biomass production, aggregate dynamics, and erosive transport; regional SOC often co-varies with broad MAP bands (e.g., near-optimal 1200–1600 mm), whereas deficits (< 800 mm) and excesses (> 3000 mm) increase vulnerability via drought stress, leaching, or erosion [64], [65].

Finally, soil pH is weighted lower because it primarily modulates microbial community composition and exoenzyme efficiency rather than directly adding stabilization capacity [43], [44]. Near-neutral pH maximizes heterotrophic respiration and carbon turnover [66], [67], which explains the high-risk expression of neutral-slightly acidic classes in valley sectors.

3.5 Parameter interrelationships and emergent behavior

Beyond single-factor effects, the SOM-LVI reveals important interactions: Clay × Temperature/pH. Where clay is low-to-moderate (10–35%), warm and near-neutral conditions accelerate decomposition without a compensatory increase in mineral protection, amplifying

vulnerability [31], [43], [50]. Andisols are a counterexample: despite warm sectors in places, their short-range-order minerals can offset temperature effects via strong sorption/microaggregation [43], [54].

Slope × Precipitation. On Moderate–High slopes, even "intermediate" MAP classes may express high vulnerability because storm erosivity and flow concentration selectively export fine, C-rich particles [34], [52]. Conversely, in low-slope valley bottoms, high MAP primarily influences mineralization/leaching rather than physical export, unless cover is sparse.

Life zone × Management. In life zones with high productivity potential, management determines whether residues feed stable MAOM pools or are rapidly mineralized/eroded. Frequent traffic, residue removal, and conventional tillage reduce inputs to MAOM and accelerate losses, whereas residue retention, cover crops, and traffic control mitigate declines [50], [51], [68], [69].

3.6 Practical implications

Moderate and High vulnerability jointly represented 97.63–100.00% of Classes 3–7, including Classes 3–6, which are especially relevant for agricultural production. This result identifies a relevant management priority because soils of considerable agricultural importance are also concentrated within the vulnerability classes that require greater attention. In Alfisol- and Mollisol-dominated production areas classified as High vulnerability, the SOM-LVI can support the prioritization of permanent soil cover, residue retention, cover crops, organic inputs, and reduced or controlled traffic. Where High vulnerability occurs on sloping terrain, these practices should be complemented with contour farming, vegetative barriers, or other measures that reduce runoff and soil redistribution [50]-[52], [68], [69].

The mapped classes should nevertheless guide the location of interventions rather than prescribe a single management practice. High-vulnerability polygons can be used to prioritize field sampling, conservation investments, and monitoring, whereas Moderate-vulnerability areas can support adaptive trials before broader implementation. Lower-vulnerability headwaters should be interpreted as areas for preventive conservation and maintenance of vegetation cover, not as areas without risk. Because current land use and management intensity were not incorporated as explicit inputs, site-specific recommendations still require field verification and information about cropping systems, tillage, residue management, and erosion conditions.

3.7 Added value of the SOM-LVI

The spatial coincidence with intensively cultivated sectors suggests that management pressure may interact with the inherent vulnerability mapped by the SOM-LVI; however, this interpretation requires field and land-management data for confirmation. Evidence from tropical and subtropical cropping systems shows that frequent traffic, residue removal, and conventional tillage reduce inputs to the mineral-associated carbon pool and accelerate losses, whereas residue retention and reduced-traffic/controlled-traffic practices mitigate declines. In practice, the SOM-LVI can guide prioritization of these interventions—e.g., enforcing residue management and cover cropping in high-risk polygons while using moderate-risk classes for adaptive trials of diversified rotations and organic amendments such as biochar [70], [71].

The added value of the SOM-LVI lies in converting six heterogeneous edaphic, topographic, and climatic parameters into a reproducible spatial prioritization surface using available semi-detailed soil cartography and climate–terrain layers. Its contribution is not limited to identifying areas with High or Moderate vulnerability. By intersecting the index with soil orders and agrological classes, the analysis identifies where potential vulnerability coincides with soils of high productive relevance and distinguishes soil–landscape combinations that may require different conservation strategies. This integration translates dispersed territorial information into a common framework that can guide sampling, monitoring, resource allocation, and soil-conservation planning. Accordingly, the SOM-LVI should be understood as a regional screening

and prioritization tool, rather than as a direct estimate of current SOM content or the amount of SOM already lost.

3.8 Limitations and improvement opportunities

The present MCDA/SAW design is transparent and operational, but several limitations merit emphasis. First, the index is essentially static: it reflects long-term climatology and mapped edaphic properties and does not capture seasonal moisture pulses, episodic storm erosivity, or management variability. Second, the SOM-LVI is sensitive to input variables, class thresholds, normalization rules, and AHP-derived weights; although the weighting scheme was literature-grounded and expert-elicited, uncertainty in expert judgment may influence the relative contribution of each parameter and, consequently, the final vulnerability classes [72], [73], [74]. Third, some drivers are represented through spatial or thematic proxies, such as life zones as an integrator of climate and soil order as an indirect proxy for mineralogical controls. Fourth, raster resolution, resampling, interpolation of temperature and precipitation, and DEM-derived slope can propagate spatial and geostatistical uncertainty into class boundaries, especially in transitional zones. Finally, the index has not yet been validated against independent field measurements of SOC, particulate organic carbon, or mineral-associated organic matter; therefore, it should be interpreted as a spatial prioritization tool rather than a predictive model of measured SOM loss.

Improvement opportunities follow directly: (i) implement formal sensitivity and uncertainty analyses to quantify the influence of weights, thresholds, and input layers; (ii) incorporate time-varying proxies, such as vegetation indices and soil moisture, to evaluate the temporal stability of vulnerability classes; (iii) couple field monitoring of SOC fractions with management metadata to test whether mapped vulnerability corresponds to observed SOM status or change; (iv) add explicit mineralogical layers, such as andic indices or clay mineralogy, where available; and (v) refine spatial inputs through geostatistical downscaling or digital soil mapping approaches [75], [76], [77]. Advancing this agenda will benefit from interdisciplinary, multi-scale, and long-term designs [78] and from continued institutional data curation.

A further verification and refinement step should include an independent field-sampling design across the main SOM-LVI classes, soil orders, and land-use types, together with the development of an exposure-adjusted SOM-LVI that incorporates current land use or land cover as a management-pressure layer.

4. CONCLUSIONS

This study operationalized and applied a GIS- and AHP-based multi-criteria index, the SOM-LVI, to assess spatial vulnerability to SOM loss in the Tuluá and La Paila river watersheds. The index produced spatial patterns consistent with known pedoclimatic gradients, revealing a predominantly Moderate–High vulnerability landscape, with High and Moderate classes covering 49.6% and 41.0% of the study area, respectively. This pattern clearly separated upper, cooler headwaters from warmer, more dissected agricultural sectors. In doing so, it delivers a transparent, reproducible tool that translates existing semi-detailed cartography and climate layers into decision-ready information for territorial planning and soil conservation.

Stratification of SOM-LVI outcomes by land-capability classes and soil taxonomic orders showed that the soil and landscape units with greatest agronomic potential also tend to concentrate the highest vulnerability, particularly Mollisols and Alfisols within Classes 3–6. Conversely, specific combinations such as Histosols and portions of Class 8 emerged as relatively less vulnerable. These contrasts provide an explicit basis for zoning: coupling intensive production and mitigation measures in high-risk soil–landscape units, while using lower-risk areas to support buffering, conservation corridors, and complementary ecosystem services. Therefore, the main practical contribution of the SOM-LVI is not only to map vulnerability, but

to identify where conservation interventions should be prioritized according to both risk level and productive relevance.

Finally, the behavior of the individual parameters highlights concrete opportunities for risk reduction. In warm areas with near-neutral pH, where conditions may favor rapid organic matter turnover, priority measures include maintaining soil cover, retaining crop residues and applying appropriate organic amendments. On steeper terrain, these measures should be complemented by practices that reduce runoff, erosion and soil redistribution. At the same time, the index remains a static, expert-weighted construct that depends on available cartography, spatial resolution, interpolation procedures, and selected input variables, and it has not yet been validated against field SOC data or temporal indicators. Future work should therefore focus on independent validation, uncertainty and sensitivity analyses, comparison of alternative weighting and normalization schemes, and the integration of management and time-varying remote-sensing proxies. These steps are necessary to move SOM-LVI from a spatial prioritization framework toward an adaptive, evidence-based tool for SOM conservation in agricultural watersheds.

5. ACKNOWLEDGMENTS AND FUNDING

The authors acknowledge the institutional funding provided by the Corporación Autónoma Regional del Valle del Cauca (CVC) and Universidad del Valle through the Inter-Administrative Contract No. 0792 of 2024 (Project Code 42061F) established between both institutions. The authors also thank the anonymous reviewers for their insightful suggestions, which substantially improved the quality and impact of this work.

6. REFERENCES

[1] L. V. da Mota Neto *et al.*, "Soil fertility matters! A new conceptual model for carbon stewardship in neotropical croplands taking climate-smart agricultural practices into account," *Sci. Total Environ.*, vol. 978, p. 179407, May. 2025. https://doi.org/10.1016/j.scitotenv.2025.179407

[2] M. Githongo *et al.*, "The structural quality of soil organic matter under selected soil fertility management practices in the Central Highlands of Kenya," *Sustainability*, vol. 15, no. 8, p. 6500, Apr. 2023. https://doi.org/10.3390/su15086500

[3] S. R. Zandoná *et al.*, "Mountain agriculture in Southeast Brazil: Soil attributes and organic matter as soil chemical quality indicators," *Catena*, vol. 259, p. 109351, Nov. 2025. https://doi.org/10.1016/j.catena.2025.109351

[4] J. M. Lavallee *et al.*, "Conceptualizing soil organic matter into particulate and mineral-associated forms to address global change in the 21st century," *Glob. Chang. Biol.*, vol. 26, no. 1, pp. 261-273, Jan. 2020. https://doi.org/10.1111/gcb.14859

[5] S. Manzoni, and M. F. Cotrufo, "Mechanisms of soil organic carbon and nitrogen stabilization in mineral-associated organic matter: Insights from modeling in phase space," *Biogeosciences*, vol. 21, no. 18, pp. 4077-4098, Sep. 2024. https://doi.org/10.5194/bg-21-4077-2024

[6] T. Sattraburut *et al.*, "Rapid decline in soil organic carbon stocks following forest-to-maize field conversion within a watershed in Northern Thailand," *Environ. Chall.*, vol. 17, p. 101042, Dec. 2024. https://doi.org/10.1016/j.envc.2024.101042

[7] G. Angst *et al.*, "Plant- or microbial-derived? A review on the molecular composition of stabilized soil organic matter," *Soil Biol. Biochem.*, vol. 156, p. 108189, May. 2021. https://doi.org/10.1016/j.soilbio.2021.108189

[8] C. Plaza *et al.*, "Physical, chemical, and biochemical mechanisms of soil organic matter stabilization under conservation tillage systems: A central role for microbes and microbial by-products in C sequestration," *Soil Biol. Biochem.*, vol. 57, pp. 124-134, Feb. 2013. https://doi.org/10.1016/j.soilbio.2012.07.026

[9] M. Shahbaz *et al.*, "Decrease of soil organic matter stabilization with increasing inputs: Mechanisms and controls," *Geoderma*, vol. 304, pp. 76-82, Oct. 2017.

https://doi.org/10.1016/j.geoderma.2016.05.019
[10] L. V. Verchot *et al.*, "Organic matter stabilization in soil aggregates: Understanding the biogeochemical mechanisms that determine the fate of carbon inputs in soils," *Geoderma*, vol. 161, no. 3-4, pp. 182-193, Mar. 2011. https://doi.org/10.1016/j.geoderma.2010.12.017
[11] M. Wiesmeier *et al.*, "Soil organic carbon storage as a key function of soils: A review of drivers and indicators at various scales," *Geoderma*, vol. 333, pp. 149-162, Jan. 2019. https://doi.org/10.1016/j.geoderma.2018.07.026
[12] K. Oechaiyaphum *et al.*, "Impact of long-term agricultural management practices on soil organic carbon and soil fertility of paddy fields in Northeastern Thailand," *Geoderma Reg.*, vol. 22, p. e00307, Sep. 2020. https://doi.org/10.1016/j.geodrs.2020.e00307
[13] R. F. Molina *et al.*, "Effects of land use change and agricultural management on soil carbon stocks in tropical pastures," *Agric. Ecosyst. Environ.*, vol. 396, p. 110024, Feb. 2026. https://doi.org/10.1016/j.agee.2025.110024
[14] C. S. S. Ferreira *et al.*, "Soil degradation in the European Mediterranean region: Processes, status and consequences," *Sci. Total Environ.*, vol. 805, p. 150106, Jan. 2022. https://doi.org/10.1016/j.scitotenv.2021.150106
[15] G. Zhu *et al.*, "Effects of land use changes on soil organic carbon, nitrogen and their losses in a typical watershed of the Loess Plateau, China," *Ecol. Indic.*, vol. 133, p. 108443, Dec. 2021. https://doi.org/10.1016/j.ecolind.2021.108443
[16] A. Hoyos-Sanclemente *et al.*, "Soil organic carbon in agricultural soils of an inter-Andean valley in Colombia: Understanding the effects of environmental and geographic variables," *Environ. Monit. Assess.*, vol. 197, no. 6, p. 697, Jun. 2025. https://doi.org/10.1007/s10661-025-14123-1
[17] M. Napoletano *et al.*, "Depletion and recovery of soil organic matter: Ecological, economic and social implications," *Ecol. Civiliz.*, vol. 2, no. 2, p. 10002, Feb. 2025. https://doi.org/10.70322/ecolciviliz.2025.10002
[18] A. Kumar *et al.*, "Recent advances in regenerative sustainable agricultural strategies for managing soil carbon and mitigating climate change consequences," *Catena*, vol. 258, p. 109208, Oct. 2025. https://doi.org/10.1016/j.catena.2025.109208
[19] R. Mitra *et al.*, "Assessment of the performance of GIS-based analytical hierarchical process (AHP) approach for flood modelling in Uttar Dinajpur district of West Bengal, India," *Geomat. Nat. Hazards Risk*, vol. 13, no. 1, pp. 2183-2226, Aug. 2022. https://doi.org/10.1080/19475705.2022.2112094
[20] V. F. Terán-Gómez *et al.*, "Integrating AHP and GIS for sustainable surface water planning: Identifying vulnerability to agricultural diffuse pollution in the Guachal River Watershed," *Sustainability*, vol. 17, no. 9, p. 4130, May. 2025. https://doi.org/10.3390/su17094130
[21] H. M. Hani *et al.*, "Sensitivity Analysis for Multi-Criteria Decision Analysis Framework for Site Selection of Aquifer Recharge with Reclaimed Water," *Sustainability*, vol. 15, no. 6, p. 5399, Mar. 2023. https://doi.org/10.3390/su15065399
[22] H. Negaresh *et al.*, "Desertification assessment using the analytic hierarchy process and GIS in Southeast Iran," *Geogr. Ann. Ser. A Phys. Geogr.*, vol. 98, no. 1, pp. 1-14, Mar. 2016. https://doi.org/10.1111/geoa.12120
[23] T. L. Saaty, "The Modern Science of Multicriteria Decision Making and its Practical Applications: The AHP/ANP Approach," *Oper. Res.*, vol. 61, no. 5, pp. 1101-1118, Sep. 2013. https://doi.org/10.1287/opre.2013.1197
[24] A. Ishizaka, "Analytic Hierarchy Process and its Extensions," in *New Perspectives in Multiple Criteria Decision Making*, M. Doumpos *et al.*, Eds., Cham, Switzerland: Springer, 2019, pp. 81-93. https://doi.org/10.1007/978-3-030-11482-4_2
[25] A. El Jazouli *et al.*, "GIS-multicriteria evaluation using AHP for landslide susceptibility mapping in Oum Er Rbia high basin (Morocco)," *Geoenviron. Disasters*, vol. 6, no. 1, p. 3, Apr. 2019. https://doi.org/10.1186/s40677-019-0119-7
[26] M. A. E. AbdelRahman *et al.*, "Enhancing land suitability assessment through integration of AHP and GIS-based for efficient agricultural planning in arid regions," *Sci. Rep.*, vol. 15, no. 1, p. 31370, Aug. 2025. https://doi.org/10.1038/s41598-025-14051-7
[27] A. F. Echeverri Sánchez *et al.*, "Vulnerabilidad de fuentes hídricas superficiales de la cuenca del río Cerrito a la contaminación difusa agrícola," *Rev. Investig. Agrar. Ambient.*, vol. 11, no. 2, pp. 117-130, Jul. 2020. https://doi.org/10.22490/21456453.3136
[28] M. Piero *et al.*, "Soil Sealing: Quantifying Impacts on Soil Functions by a Geospatial Decision Support System," *Land Degrad. Dev.*, vol. 28, no. 8, pp. 251-2526, Nov. 2017. https://doi.org/10.1002/ldr.2802
[29] E. F. Sanchez, and C. I. Alvarez, "Prioritization of Hydrological Restoration Areas Using AHP and GIS in Dulcepamba River Basin in Bolivar–Ecuador," *Hydrology*, vol. 11, no. 6, p. 81, Jun. 2024.

https://doi.org/10.3390/hydrology11060081
[30] Instituto Geográfico Agustín Codazzi, and Corporación Autónoma Regional del Valle del Cauca, *Levantamiento Semidetallado de Suelos del Departamento del Valle del Cauca Escala 1:25.000*. Ecopedia, 2025. Accessed: Jan. 22, 2025. [Online]. Available: https://ecopedia.cvc.gov.co/suelo/caracteristicas-del-suelo/levantamiento-semidetallado-de-suelos-del-departamento-del-valle
[31] M. F. Cotrufo *et al.*, "Soil carbon storage informed by particulate and mineral-associated organic matter," *Nat. Geosci.*, vol. 12, no. 12, pp. 989-994, Dec. 2019. https://doi.org/10.1038/s41561-019-0484-6
[32] M. Mayer *et al.*, "Dynamic stability of mineral-associated organic matter: Enhanced stability and turnover through organic fertilization in a temperate agricultural topsoil," *Soil Biol. Biochem.*, vol. 184, p. 109095, Sep. 2023. https://doi.org/10.1016/j.soilbio.2023.109095
[33] Z. Zhou *et al.*, "Global turnover of soil mineral-associated and particulate organic carbon," *Nat. Commun.*, vol. 15, no. 1, p. 5329, Dec. 2024. https://doi.org/10.1038/s41467-024-49743-7
[34] S. Doetterl *et al.*, "Erosion, deposition and soil carbon: A review of process-level controls, experimental tools and models to address C cycling in dynamic landscapes," *Earth-Sci. Rev.*, vol. 154, pp. 102-122, Mar. 2016. https://doi.org/10.1016/j.earscirev.2015.12.005
[35] G. R. Hancock *et al.*, "Soil erosion and carbon export: A case study in a steep slope grazing landscape," *Geoderma Reg.*, vol. 36, p. e00751, Mar. 2024. https://doi.org/10.1016/j.geodrs.2023.e00751
[36] F. Gou *et al.*, "Decrease in Erosion-Induced Soil Organic Carbon as a Result of Vegetation Restoration in the Loess Plateau, China," *J. Geophys. Res. Biogeosci.*, vol. 127, no. 8, p. e2022JG006917, Aug. 2022. https://doi.org/10.1029/2022JG006917
[37] H. F. Jungkunst *et al.*, "New uses for old tools: Reviving Holdridge Life Zones in soil carbon persistence research," *J. Plant Nutr. Soil Sci.*, vol. 184, no. 1, pp. 5-11, Feb. 2021. https://doi.org/10.1002/jpln.202100008
[38] S. F. von Fromm *et al.*, "Moisture and soil depth govern relationships between soil organic carbon and oxalate-extractable metals at the global scale," *Biogeochemistry*, vol. 168, no. 1, p. 20, Feb. 2025. https://doi.org/10.1007/s10533-025-01208-9
[39] T. W. Crowther *et al.*, "Quantifying global soil carbon losses in response to warming," *Nature*, vol. 540, no. 7631, pp. 104-108, Dec. 2016. https://doi.org/10.1038/nature20150
[40] Y. Chen *et al.*, "Long-term warming reduces surface soil organic carbon by reducing mineral-associated carbon rather than 'free' particulate carbon," *Soil Biol. Biochem.*, vol. 177, p. 108905, Feb. 2023. https://doi.org/10.1016/j.soilbio.2022.108905
[41] H. Guo *et al.*, "Mapping surface soil organic carbon density of cultivated land using machine learning in Zhengzhou," *Environ. Geochem. Health*, vol. 47, no. 1, Jan. 2025. https://doi.org/10.1007/s10653-024-02313-8
[42] Q. W. Li *et al.*, "Precipitation patterns impact soil aggregates and organic carbon of an alpine wetland on the Qinghai-Tibetan Plateau," *Catena*, vol. 244, p. 108249, Sep. 2024. https://doi.org/10.1016/j.catena.2024.108249
[43] E. W. Slessarev *et al.*, "Water balance creates a threshold in soil pH at the global scale," *Nature*, vol. 540, no. 7634, pp. 567-569, Dec. 2016. https://doi.org/10.1038/nature20139
[44] J. Puissant *et al.*, "The pH optimum of soil exoenzymes adapt to long term changes in soil pH," *Soil Biol. Biochem.*, vol. 138, p. 107601, Nov. 2019. https://doi.org/10.1016/j.soilbio.2019.107601
[45] L. Abdullah, and C. W. R. Adawiyah, "Simple additive weighting methods of multi criteria decision making and applications: A decade review," *Int. J. Inf. Process. Manag.*, vol. 5, no. 1, pp. 39-49, Feb. 2014. https://pdfs.semanticscholar.org/05a0/d6d88b7a86fd783f736532af68e0e297e299.pdf
[46] I. Kaliszewski, and D. Podkopaev, "Simple additive weighting—A metamodel for multiple criteria decision analysis methods," *Expert Syst. Appl.*, vol. 54, pp. 155-161, Jul. 2016. https://doi.org/10.1016/j.eswa.2016.01.042
[47] H. Taherdoost, "Analysis of simple additive weighting method (SAW) as a multi-attribute decision-making technique: A step-by-step guide," *J. Manag. Sci. Eng. Res.*, vol. 6, no. 1, pp. 21-24, Feb. 2023. https://doi.org/10.30564/jmser.v6i1.5400
[48] T. Ewunetu *et al.*, "Soil properties under different land uses and slope gradients: Implications for sustainable land management in the Tach Karnuary watershed, Northwestern Ethiopia," *Front. Environ. Sci.*, vol. 13, p. 1518068, May. 2025. https://doi.org/10.3389/fenvs.2025.1518068
[49] K. Georgiou *et al.*, "Global stocks and capacity of mineral-associated soil organic carbon," *Nat. Commun.*, vol. 13, no. 1, p. 3797, Dec. 2022. https://doi.org/10.1038/s41467-022-31540-9
[50] E. E. Oldfield *et al.*, "Global meta-analysis of the relationship between soil organic matter and crop yields," *Soil*, vol. 5, no. 1, pp. 15-32, Jan. 2019. https://doi.org/10.5194/soil-5-15-2019

[51] J. L. N. Carvalho *et al.*, "Agronomic and environmental implications of sugarcane straw removal: A major review," *GCB Bioenergy*, vol. 9, no. 7, pp. 1181-1195, Jul. 2017. https://doi.org/10.1111/gcbb.12410

[52] L. Wang *et al.*, "Effects of the rainfall intensity and slope gradient on soil erosion and nitrogen loss on the sloping fields of Miyun Reservoir," *Plants*, vol. 12, no. 3, p. 423, Jan. 2023. https://doi.org/10.3390/plants12030423

[53] T. Li *et al.*, "Soil erosion affects variations of soil organic carbon and soil respiration along a slope in Northeast China," *Ecol. Process.*, vol. 8, no. 1, p. 28, Aug. 2019. https://doi.org/10.1186/s13717-019-0184-6

[54] S. Anindita *et al.*, "Tropical Andosol organic carbon quality and degradability in relation to soil geochemistry as affected by land use," *Soil*, vol. 9, no. 2, pp. 443-459, Jul. 2023. https://doi.org/10.5194/soil-9-443-2023

[55] M. Kleber *et al.*, "Mineral–organic associations: Formation, properties, and relevance in soil environments," in *Advances in Agronomy*, *vol. 130*, D. L. Sparks, Ed., Cambridge, MA, USA: Academic Press, 2015, ch. 1, pp. 1-140. https://doi.org/10.1016/bs.agron.2014.10.005

[56] A. Johannes *et al.*, "Soil organic carbon content and soil structure quality of clayey cropland soils: A large-scale study in the Swiss Jura region," *Soil Use Manag.*, vol. 39, no. 2, pp. 707-716, Apr. 2023. https://doi.org/10.1111/sum.12879

[57] J. M. Prout *et al.*, "Changes in organic carbon to clay ratios in different soils and land uses in England and Wales over time," *Sci. Rep.*, vol. 12, no. 1, p. 5162, Mar. 2022. https://doi.org/10.1038/s41598-022-09101-3

[58] J. Ling *et al.*, "Soil organic carbon thresholds control fertilizer effects on carbon accrual in croplands worldwide," *Nat. Commun.*, vol. 16, no. 1, p. 3009, Mar. 2025. https://doi.org/10.1038/s41467-025-57981-6

[59] D. Kabelka *et al.*, "Reduction in soil organic matter loss caused by water erosion in inter-rows of hop gardens," *Soil Water Res.*, vol. 14, no. 3, pp. 172-182, Sep. 2019. https://doi.org/10.17221/135/2018-SWR

[60] A. Komarova *et al.*, "Temperature Sensitivity of topsoil Organic Matter Decomposition Does Not Depend on Vegetation Types in Mountains," *Plants*, vol. 11, no. 20, p. 2765, Oct. 2022. https://doi.org/10.3390/plants11202765

[61] F. C. Santos *et al.*, "Organic matter: A critical soil health indicator in agrosystems within the Cerrado of Bahia, Brazil and South Florida, USA," *Front. Soil Sci.*, vol. 5, p. 1524550, May. 2025. https://doi.org/10.3389/fsoil.2025.1524550

[62] S. Ren *et al.*, "Projected soil carbon loss with warming in constrained Earth system models," *Nat. Commun.*, vol. 15, no. 1, p. 102, Jan. 2024. https://doi.org/10.1038/s41467-023-44433-2

[63] E. A. Davidson, and I. A. Janssens, "Temperature sensitivity of soil carbon decomposition and feedbacks to climate change," *Nature*, vol. 440, pp. 165-173, Mar. 2006. https://doi.org/10.1038/nature04514

[64] L. M. Wahab *et al.*, "Carbon and nitrogen dynamics in subsoils after 20 years of added precipitation in a Mediterranean grassland," *Biogeosciences*, vol. 22, no. 15, pp. 3915-3930, Aug. 2025. https://doi.org/10.5194/bg-22-3915-2025

[65] S. Xu *et al.*, "Precipitation change affects forest soil carbon inputs and pools: A global meta-analysis," *Sci. Total Environ.*, vol. 908, p. 168171, Jan. 2024. https://doi.org/10.1016/j.scitotenv.2023.168171

[66] H. Cao *et al.*, "Soil pH, total phosphorus, climate and distance are the major factors influencing microbial activity at a regional spatial scale," *Sci. Rep.*, vol. 6, p. 25815, May. 2016. https://doi.org/10.1038/srep25815

[67] C. Pan *et al.*, "Microbial community interactions determine the mineralization of soil organic phosphorus in subtropical forest ecosystems," *Microbiol. Spectr.*, vol. 12, no. 3, p. e01355-23, Mar. 2024. https://doi.org/10.1128/spectrum.01355-23

[68] M. R. Cherubin *et al.*, "Soil Quality Indexing Strategies for Evaluating Sugarcane Expansion in Brazil," *PLoS One*, vol. 11, no. 3, p. e0150860, Mar. 2016. https://doi.org/10.1371/journal.pone.0150860

[69] P. Smith *et al.*, "How to measure, report and verify soil carbon change to realize the potential of soil carbon sequestration for atmospheric greenhouse gas removal," *Glob. Chang. Biol.*, vol. 26, no. 1, pp. 219-241, Jan. 2020. https://doi.org/10.1111/gcb.14815

[70] B. Minasny *et al.*, "Soil carbon 4 per mille," *Geoderma*, vol. 292, pp. 59-86, Apr. 2017. https://doi.org/10.1016/j.geoderma.2017.01.002

[71] D. Guarín *et al.*, "Biochar for climate change mitigation and soil health management," in *Biochar Ecotechnology for Sustainable Agriculture and Environment*, A. Kumar *et al.*, Eds., Amsterdam, The Netherlands: Elsevier, 2025, ch. 9, pp. 231-259. https://doi.org/10.1016/B978-0-443-29855-4.00011-4

[72] M. Cinelli *et al.*, "How to support the application of multiple criteria decision analysis? Let us start with a comprehensive taxonomy," *Omega*, vol. 96, p. 102261, Oct. 2020.

https://doi.org/10.1016/j.omega.2020.102261
[73] R. O'Shea *et al.*, "Weight stability intervals for multi-criteria decision analysis using the weighted sum model," *Expert Syst. Appl.*, vol. 296, Part B., p. 128460, Jan. 2026. https://doi.org/10.1016/j.eswa.2025.128460
[74] S. Bandyopadhyay, "A novel multi-criteria decision analysis technique incorporating demanding essential characteristics of existing MCDA techniques," *Prog. Artif. Intell.*, vol. 12, no. 3, pp. 231-255, Sep. 2023. https://doi.org/10.1007/s13748-023-00299-5
[75] G. Demir *et al.*, "Sensitivity analysis in multi-criteria decision making: A state-of-the-art research perspective using bibliometric analysis," *Expert Syst. Appl.*, vol. 237, Part C, p. 121660, Mar. 2024. https://doi.org/10.1016/j.eswa.2023.121660
[76] J. Padarian *et al.*, "Using deep learning for digital soil mapping," *Soil*, vol. 5, no. 1, pp. 79-89, Feb. 2019. https://doi.org/10.5194/soil-5-79-2019
[77] R. A. Viscarra Rossel *et al.*, "A global spectral library to characterize the world's soil," *Earth-Sci. Rev.*, vol. 155, pp. 198-230, Apr. 2016. https://doi.org/10.1016/j.earscirev.2016.01.012
[78] S. D. Keesstra *et al.*, "European agricultural soil management: Towards climate-smart and sustainability, knowledge needs and research approaches," *Eur. J. Soil Sci.*, vol. 75, no. 1, p. e13437, Jan. 2024. https://doi.org/10.1111/ejss.13437

CONFLICT OF INTEREST

The authors declare no conflicts of interest related to this manuscript.

AUTHORSHIP CONTRIBUTION

Clever Gustavo Becerra-Romero: Conceptualization, Methodology and Acquisition of data.

Andrés Fernando Echeverri-Sánchez: Research management, Conceptualization, Methodology, Formal Analysis, and Investigation.

Jhony Armando Benavides-Bolaños: Formal Analysis, Data Visualization, Writing Original Draft, and Editing Final Draft.

María del Mar Carreño-Sánchez: Methodology, Formal Analysis, and Data visualization.

DECLARATION OF GENERATIVE AI AND AI-ASSISTED TECHNOLOGIES

During the preparation of this work the authors used ChatGPT v5.1 (https://openai.com/) in order to avoid grammatical and typographical errors of the English text. After using this tool/service, the authors reviewed and edited the content as needed and take full responsibility for the content of the published article.